Jurnal Fisika Flux: Jurnal Ilmiah Fisika FMIPA Universitas Lambung Mangkurat
Volume 23, Nomor 1, Februari 2026
1819-796X (p-ISSN); 2541-1713 (e-ISSN)
https://ppjp.ulm.ac.id/journal/index.php/f *Research Article*

Performance of H-ZSM-5/TiO_2 Nanocatalyst on Green Biodiesel Synthesis from Tobacco Seed Oil *(Voor-Oogst and Na-Oogst)* as Renewable Energy

Sri Wahyuni[1,*)], Sri Rahmawati[2)], Muhammad Rusdi[3)], M. Ikhwan Najmi[4)], Irving Dahlan Saksak[1)]
[1)] Department of Agricultural Products Technology, Universitas Kristen Cipta Wacana, Malang, Indonesia, 071029
[2)] Department of Mechanical Engineering, Universitas Kristen Cipta Wacana, Malang, Indonesia, 071029
[3)] Al Hamra High School, Islamic Boarding School of Al Hamra, Malang, Indonesia, 65151
[4)] Departement of Physic, Universitas Lambung Mangkurat, Banjarmasin, 70123

Email korespondensi : sriwahyuni@cwcu.ac.id

DOI: https://doi.org/10.20527/flux.v23i1.24024

Submitted: 27 September 2025; Revised: 4 March 2026; Accepted: 5 March 2026

ABSTRACT

Based on the seasons in Indonesia, tobacco is classified into two types: cigar tobacco (Na-Oogst) and cigarette or kretek tobacco (Voor-Oogst). Tobacco seeds contain around 36-41% oil, which has the potential to be a renewable energy source. Biodiesel is one of the renewable alternative energy sources that has received much attention because it is a clean and green energy. Biodiesel is produced from triglycerides through a transesterification reaction with homogeneous and heterogeneous catalysts. Heterogeneous catalysts are more attractive because they can be regenerated and are environmentally friendly. The advantages of this catalyst are that it has good catalytic activity due to its large surface area and superior stability. Zeolite H-ZSM-5 appears as a solid acid catalyst with a promising microporous structure for esterification and transesterification reactions. In this study, TiO_2 doping was added to improve the performance of the H-ZSM-5 catalyst. TiO_2 is a leading photocatalyst because it has chemical, biological, and non-toxic stability. Furthermore, to determine the success of the synthesis of H-ZSM-5/TiO_2 as a nanocatalyst, XRD, FTIR, SEM-EDX Mapping characterization was carried out. The results showed that the addition of TiO_2 which has a particle size distribution of 46.07 nm in the synthesis of H-ZSM-5/TiO_2 did not cause changes in structure and degree of crystallinity. The experimental parameters of transesterification that were varied were catalyst concentration. The results of the transesterification reaction yielded the highest methyl ester of 87.5% at optimum reaction conditions and a catalyst concentration of 2% w/w with a molar ratio of oil and methanol (1:12). The synthesized methyl ester has a characterization value that enters the range of SNI biodiesel values, so that the synthesized methyl ester has the potential to be used as biodiesel. We hope that this research can inspire researchers related to heterogeneous nanocatalyst research that is more efficient and rational and has good stability in the production of sustainable renewable fuels.

KATA KUNCI: Performance, H-ZSM-5/TiO_2, Green Synthesis, Tobacco Seed Oil, Renewable Energy.

INTRODUCTION

Fossil fuels have become the world's primary energy source. Some scientists predict that fossil fuels will be ineffective as future fuels due to their limited supply, rising prices, global warming, and environmental pollution (Jit Sarma *et al.*, 2023). Concerns about the depletion of fossil fuels have spread worldwide, including in Indonesia. Therefore, the development of renewable, environmentally friendly, and economical energy sources is intensifying. One focus of

renewable energy development in Indonesia is biodies (El-Naggar *et al.,* 2024). Biodiesel is a methyl ester of long-chain fatty acids that can be produced by transesterification of animal and vegetable oils, such as Tobacco Seed Oil (TSO) (Duraisamy *et al.,* 2025; Matheos *et al.,* 2023). Based on the seasons in Indonesia, tobacco is classified into two types: cigar tobacco (Na-Oogst) and cigarette or kretek tobacco (Voor-Oogst). Tobacco seeds contain approximately 36-41% vegetable oil, which has the potential to be a renewable energy source (Fatica *et al.,* 2025). Although biodiesel from vegetable oil has long been developed, reliance on liquid homogeneous catalysts still creates new environmental problems in the form of washing waste (Santoso *et al.,* 2021).

On the other hand, conventional heterogeneous catalysts are often less efficient at handling oils with complex characteristics. Until now, the potential of tobacco seed oil varieties (Voor-Oogst) and (Na-Oogst) has not been fully explored as a biodiesel feedstock, especially in relation to the use of H-ZSM-5/TiO_2 nanocatalysts. The synergy between the zeolite pore structure and the surface activity of nano TiO_2 is predicted to increase stability and conversion yield. However, scientific data on the comparative performance of the two tobacco varieties in this catalytic system is still very limited (Mojapelo *et al.,* 2025).

The zeolite favored as a catalyst in the transesterification reaction is ZSM-5 (Zeolite Secony Mobile-5). In addition to its unique and extraordinary properties, ZSM-5 also has a pore diameter of 0.56 nm. ZSM-5 is also a heterogeneous catalyst with Bronsted and Lewis acid sites (Yang *et al.,* 2023). Therefore, activation of ZSM-5 with H_2SO_4 is important to carry out a nucleophilic substitution reaction that converts carboxylic acids or a carboxylic acid derivative from vegetable oils and alcohols into an ester using the acid catalyst H-ZSM-5. Heterogeneous acid catalysts may be less active but more stable than heterogeneous base catalysts in the degradation of free fatty acids (Ahmad *et al.,* 2025). This study aligns with previous studies showing that adding acid to porous materials can increase surface area and catalytic performance. However, in improving performance, this catalyst needs to be doped with a transition metal (Tshabalala 2025). One of the transition metals used as a support for H-ZSM-5 is titanium dioxide.

TiO_2 nanoparticles exhibit two phases, namely rutile and anatase, with band gaps of 3.0 eV and 3.2 eV, respectively. The anatase phase of TiO_2 nanomaterial was chosen because it has a band gap of 3.2 eV (Zeleke and Tefera 2024). In addition, the wide band gap of TiO_2 nanoparticles enables them to degrade triglycerides into methyl esters by reducing their molecular weight under UV irradiation. In contrast to the general use of TiO_2 as a photocatalytic agent, in this study TiO_2 functioned as a Lewis acid site promoter and surface modifier (Jit Sarma *et al.,* 2023). The presence of TiO_2 on the H-ZSM-5 support is predicted to increase the density of active sites and improve the adsorption characteristics of large triglyceride molecules from tobacco seed oil, thereby increasing conversion efficiency (Simhadri *et al.,* 2024).

Transesterification reactions are generally carried out conventionally, so they require a fairly long time, between 1 and 3 hours (Santoso *et al.,* 2021). Research conducted on biodiesel synthesis using conventional methods lasted for 1 hour. The long reaction times in conventional methods can be overcome by using ultrasonic waves in esterification and transesterification reactions (Rajesh *et al.,* 2024). The use of ultrasonic waves in biodiesel synthesis from tobacco seed oil was previously carried out by Santoso, A., *et al.* (2021), in their research requiring an optimum reaction time of 1-10 minutes, so that the reaction time is faster and more efficient. Based on the description above, it is necessary to research the transesterification of tobacco seed oil (Voor-Oogst and Na-Oogst) using a heterogeneous catalyst, H-ZSM-5/ TiO_2, under UV irradiation assisted by ultrasonic waves. The purpose of this research is to study the main product of the reaction, biodiesel, from tobacco seed oil (Voor-Oogst and Na-Oogst), and to provide scientific development in the field of heterogeneous catalysis to support

sustainable green energy.

MATERIALS AND METODS

Materials

TSO was obtained from the extraction of tobacco seed oil. Tobacco type (Voor-Oogst) came from Paiton District, Probolinggo Regency, East Java, and tobacco type (Na-Oogst) came from Besuki District, Situbondo Regency, East Java. TSO extraction used n-hexane solvent. The ZSM-5 activation process included deionized water, Whatman No. 42 filter paper, and H_2SO_4 p.a (Merck) to activate the zeolite surface. To develop the H-ZSM-5/TiO_2 photocatalyst, 15% $TiCl_3$ Sigma-Aldrich, 12 M HCl (Merck), 6.5 M NH_4OH (Merck), deionized water, ethanol p.a., and distilled water were used. The transesterification process used methanol p.a., a 200 W UV lamp (λ < 387 nm), and characterization tests included KOH (Merck) material, pp indicator, acetone, and washing with demineralized water. All chemicals were used as intended without further modification or adjustment.

Synthesis of TiO_2 Nanoparticles

TiO_2 synthesis was carried out by the coprecipitation method, namely mixing 5 mL of 15% $TiCl_3$ with 5 mL of 12 M HCl and 15 mL of deionized water and stirring for 60 min. Then, 25 mL of 6.5 M NH_4OH was added slowly, and the mixture was stirred at 720 rpm using a magnetic stirrer for 90 min. After that, it was washed with distilled water until the pH was 7. Then it was oven-dried at 100 ^oC for 1 hour and calcined for 3 hours at 500 ^oC.

Activation of Zeolite H-ZSM-5

The ZSM-5 zeolite was washed with deionized water and stirred for 15 minutes. Then it was filtered through a Buchner funnel under vacuum. The filtered results were oven-dried for 1 hour, calcined for 3 hours at 500 °C, added to 15% H_2SO_4 while stirring for 1 hour, and left for 24 hours. The mixture was filtered under vacuum using a Buchner funnel and washed until the pH reached 7. The filtered results were then oven-dried at 100 ^oC for 2 hours and calcined at 500 ^oC for 5 hours.

Synthesis of H-ZSM-5/TiO_2 Nanocatalyst

Weighed 1.5 g of anatase TiO_2 and sonicated for 30 minutes. Finally, 1.5 g of functionalized H-ZSM-5 was added to the mixture, followed by sonication for 60 minutes. The resulting mixture was filtered through a Buchner funnel and dried at 100 °C for 3 hours. The resulting nanocomposite was heated to 500 °C in a furnace.

Soxhlet Extraction TSO

The tobacco seed mixture was dried in the sun. Then, it was ground until smooth. A total of 70 g of dried tobacco seed powder was extracted by Soxhlet extraction using n-hexane until the solvent returned to colorless, approximately 60 minutes later. The extraction was repeated every 70 g of sample until sufficient oil was obtained for the transesterification process. The oil extract, still mixed with the solvent, was evaporated using a rotary vacuum evaporator (rotavapor).

Green Biodiesel Synthesis

The transesterification process uses a mole ratio of oil to methanol of 1:12. Place 20 g in a three-neck flask and heat to 100 °C for 15 minutes. After heating is complete, lower the oil temperature to 64°C. Add methanol and the H-ZSM-5/TiO_2 catalyst at varying concentrations (1, 1.5, 2%) w/w oil. The mixture is placed in an ultrasonic cleaner for 5 minutes under UV light. After that, it is filtered with a vacuum Buchner funnel and into a separating funnel and left for ± 24 hours. The resulting methyl ester is stirred and heated to ± 100 °C to remove water.

RESULTS AND DISCUSSION

Diffraction Peak Analysis of H-ZSM-5/ TiO_2 Nanocatalyst

The XRD pattern of H-ZSM-5/TiO_2 nanocatalyst is shown in Figure 1. The XRD pattern of H-ZSM-5 was detected at 2 theta peaks of 16.40°, 21.05°, 24.43°, 25.06°, 27.41°, 29.65° and 34.07° (Yang *et al.*, 2023). These peaks correspond to (AMCSD 0010960) zeolite

(ZSM-5). This is also in accordance with previously reported data. The existence of TiO_2 crystals in the hkl plane is as follows: (101), (103), (104), (112), (200), (105), (211), (204) (Muniyappan and Krishnaiah 2024). The XRD pattern of H-ZSM-5/TiO_2 shows the characteristic peaks of the nanocomposite's constituent materials, namely zeolite ZSM-5 and TiO_2. Furthermore, the peak intensity of H-ZSM-5 and TiO_2 decreases and broadens with increasing H-ZSM-5 mass. According to previous researchers, the intensity is proportional to the number of crystals. The following are the results of the H-ZSM-5/ TiO_2 nanocomposite refinement. Based on the refinement results, they can be seen in Table 1.

Table 1. Refinement results of H-ZSM-5/TiO_2 nanocomposite

Parameter	H-ZSM-5	TiO_2
Rp	21,25	20,31
Rwp	27,47	26,23
X^2	1,22	1,27
Bragg R-Factor	9,18	10,03
Lattice (Å)		
($a = b = c$)	20,0;19,9;13,3	
($a = b \neq c$)		3,781; 9,512
Unit Cell Volume (Å³)	5332	137

Based on the results of Rietveld analysis using Rietica software, statistical indicator values that meet the reliability criteria are obtained, namely, low Rp, Rwp, and X2 values. This indicates that the proposed structural model provides a very good fit to the experimental diffraction data (Zhou *et al.*, 2025). Figure 1 shows an increase in the diffraction peak intensity with increasing H-ZSM-5 mass. Based on the literature, these results are consistent with previous studies. Changes in the position of the diffraction angle are influenced by the presence of TiO_2 nanoparticles on the surface of H-ZSM-5.

In Figure 1, the TiO_2 diffraction peak is almost completely invisible. This is due to the overlapping peak with the ZSM-5 diffraction peak. In addition, the nanocomposite particle size value decreases when the mass of one of the nanocomposite materials is varied (Yang *et al.*, 2023). This decrease in particle size indicates that the nanocomposite surface has been dispersed with TiO_2 nanoparticles as a coating, resulting in an even distribution of bonds. Zeolite functions as a matrix in the nanocomposite. As a result, the nanocomposite becomes uniform and homogeneous.

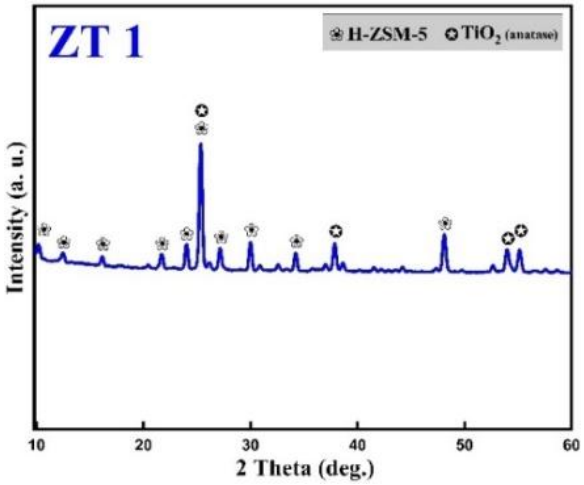

Figure 1. XRD Analysis Results of Nanocatalyst H-ZSM-5/TiO_2

Functional Group of H-ZSM-5/TiO_2 Nanocatalyst

The addition of TiO_2 to the nanocomposite structure will produce Ti-O-Ti functional groups at 456 and 544 cm^{-1} (El-Kady *et al.*, 2021). Furthermore, the presence of a band at 1614 cm-1 is caused by the presence of OH functional groups from water molecules. The band at 1215 cm^{-1} is associated with the Si-O-T (T= Si, Al) chain of the zeolite group (Stepanov *et al.*, 2023). The band around 816 cm^{-1} is the O-T-O (T= Si, Al) stretching and bending vibration of condensed silica. These results have been confirmed in previous studies. In addition, the transmittance decreases with increasing H-ZSM-5 fraction in the nanocatalyst.

That data provides evidence that the zeolite structure remains unchanged after coating with TiO_2. However, it should be noted that the wave numbers of TiO_2 and ZSM-5 are very close in the FTIR spectrum. So the Ti-O-Ti band is not clearly visible in the FTIR spectrum of the H-ZSM-5/TiO_2 nanocatalyst, as in Figure 2. In addition, the appearance of vibration peaks at wave numbers 1044 cm^{-1} indicates the formation of Si(Al)-O-Si(Al) bonds, and 1215

cm^{-1} indicates the formation of C-H bonds. Next, there is a vibration peak at wave number 3188 cm^{-1} originating from the Si-OH-Al functional group (Ahmad *et al.*, 2025). This functional group arises because water molecules are trapped in the H-ZSM-5 cavity of the nanocomposite. Based on the mass analysis of H-ZSM-5, which is more dominant in the nanocomposite sample, the Ti-O-Ti bonds in the nanocatalyst are not detected (Simhadri *et al.*, 2024). This may be due to the nanocomposite being successfully coated with H-ZSM-5 particles, so that the Ti-O-Ti functional groups overlap with the H-ZSM-5 functional groups.

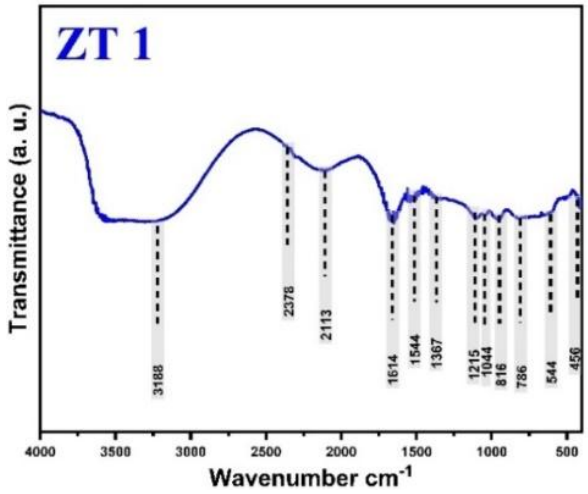

Figure 2. FTIR Analysis Results of H-ZSM-5/TiO_2 Nanocatalyst

All nanocomposite samples exhibited Si-O-Al functional group bands at 786 cm^{-1}, indicating the H-ZSM-5 content in the nanocatalyst matrix. Furthermore, there were vibration peaks at 2378 cm^{-1}, which indicated the presence of Si-O bonds, and at 2113 cm^{-1}, which indicated the formation of CO_2 molecular bonds in the air. There was also an O-H functional group bond at a wave number of 1514 cm^{-1} (Ahmad et al., 2025). The presence of an O-H functional group bond indicated that water molecules adsorbed on the surface of the nanocatalyst sample. On the other hand, bending vibrations of water molecules adsorbed in the zeolite pores or bound to cations were observed at 1614 cm^{-1}. The O-H functional group bond can also indicate the presence of Si-OH-Al groups. The composition of this compound can improve the performance of the H-ZSM-5/TiO_2 nanocatalyst in its use for the conversion of vegetable oil into biodiesel.

Morphology of H-ZSM-5/TiO_2 Nanocatalyst

The morphology and particle size distribution of the H-ZSM-5/TiO_2 nanocatalyst were characterized by SEM, as shown in Figure 3 at a magnification of 60,000. Based on qualitative analysis, the H-ZSM-5/TiO_2 nanocomposite tends to agglomerate. Theoretically, the phenomenon of the tendency for agglomeration of the H-ZSM-5/ TiO_2 nanocatalyst is caused by the higher mass composition of TiO_2 in the nanocomposite compared to the mass of H-ZSM-5. This is also influenced by the decrease in kinetic energy resulting from collisions between nanocatalyst particles. Conversely, a decrease in TiO_2 mass reduces the agglomeration rate of the H-ZSM-5/ TiO_2 nanocatalyst. This is because TiO_2 has a particle size distribution of around 40-50 nm. This size promotes strong interactions between TiO_2 particles in the nanocomposite. The particle size distribution of the nanocomposite, obtained using the ImageJ application, is presented in Figure 3.

Furthermore, the decreased agglomeration rate can be attributed to the TiO_2 particles being evenly distributed over the surface of H-ZSM-5. Nanocatalysts that have not been coated with adhesive will have weaker interactions, resulting in agglomerates, and the resulting intermolecular forces will be stronger, leading to agglomeration (Khatrin *et al.*, 2025). Then, when the nanocomposite is added with H-ZSM-5, layers with non-magnetic properties will form on each particle surface. As a result, the agglomeration rate of the nanocatalyst is reduced, leading to a decrease in the particle size distribution (Simhadri *et al.*, 2024). On the other hand, the addition of TiO_2 nanoparticles will increase the homogeneity of the nanocatalyst sample and improve its stability.

Furthermore, the decreased agglomeration rate can be attributed to the TiO_2 particles being evenly distributed over the surface of H-ZSM-5. Nanocatalysts that have not been coated with

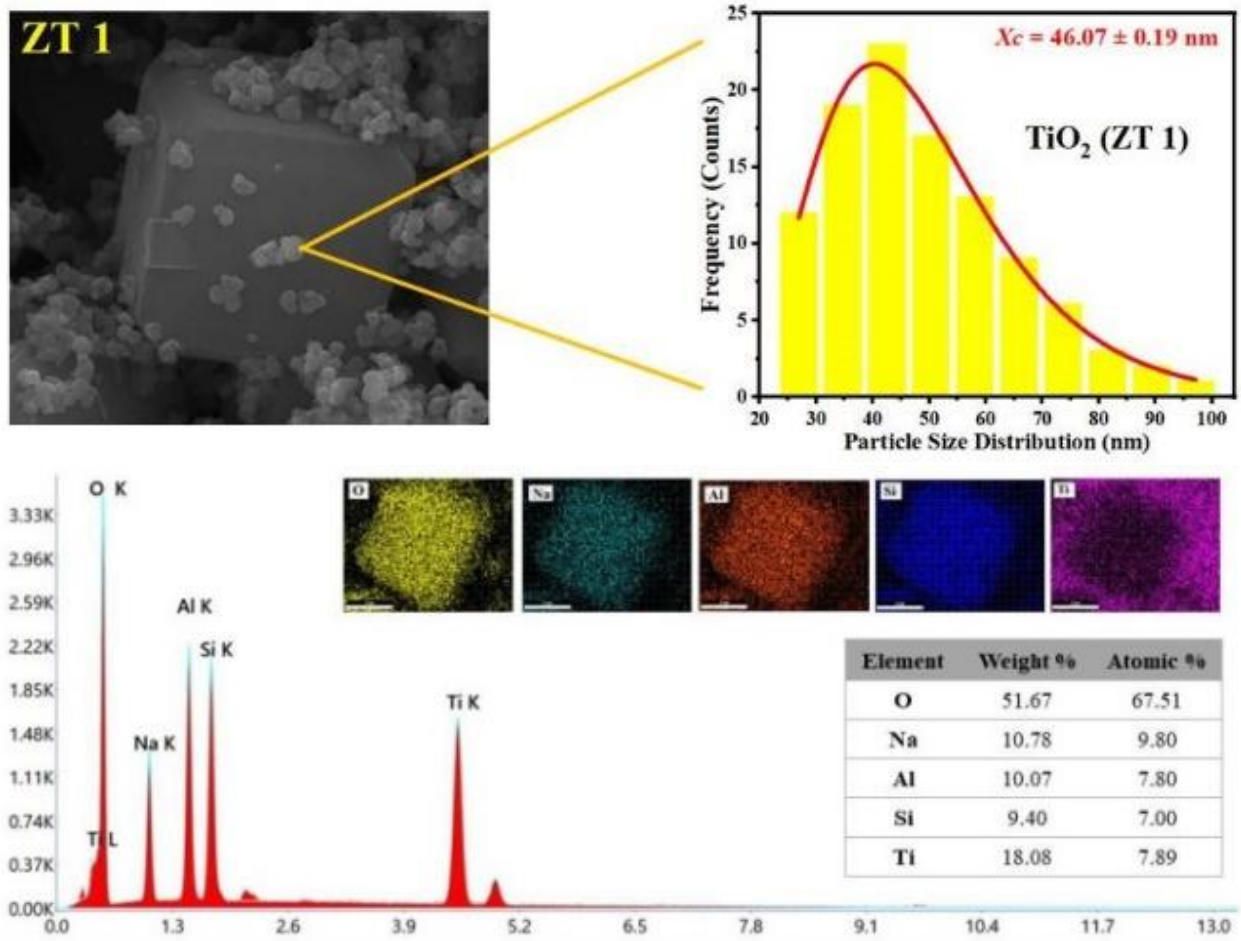

Figure 3. SEM-EDX Mapping Analysis and Particle Size Distribution of H-ZSM-5/TiO_2 Nanocatalyst

adhesive will have weaker interactions, resulting in agglomerates, and the resulting intermolecular forces will become stronger, leading to agglomeration. Then, when the nanocomposite is added with H-ZSM-5, layers with non-magnetic properties will form on each particle surface (Simhadri *et al.*, 2024). As a result, the agglomeration rate of the nanocatalyst is reduced, leading to a decrease in the particle size distribution. On the other hand, the addition of TiO_2 nanoparticles will improve the homogeneity of the nanocatalyst sample and increase its stability (Shinnur *et al.*, 2024).

Performance of H-ZSM-5/TiO_2 Nanocatalyst on Biodiesel Yield

The synthesis of methyl ester from tobacco seed oil is based on the transesterification reaction of a new ester with methanol using H-ZSM-5/ TiO_2 nanocatalyst to form a new ester and a new alcohol. Ultrasonic waves assist this synthesis. The first step is to heat the oil to ±100 °C. Then add a mixture of oil and methanol with a ratio of 1:12 and variations in the concentration of the H-ZSM-5/TiO_2 catalyst (1; 1.5; 2)% w/w oil. In this esterification and transesterification reaction, the reaction time is 1 to 10 minutes. The reaction mechanism for the esterification and transesterification of tobacco seed oil is shown in Figure 4.

At this stage, the fatty acids interact with the surface of the H-ZSM-5/TiO_2 catalyst. UV light excites electrons in TiO_2, creating active sites. Protons (H+) from the zeolite catalyst (H-ZSM-5) attack the oxygen on the carbonyl group of the fatty acid, forming a positively charged intermediate (carbocation) (Ansari *et al.*, 2025). The methanol molecule then attacks the positively charged central carbon atom. At this stage, methanol is incorporated into the structure, forming an intermediate complex in which the carbon atom binds to an -R group, two -OH groups, and one -OCH_3 group that still carries a proton. A proton transfer occurs within the molecule, causing one of the hydroxyl groups (-OH) to convert into a water

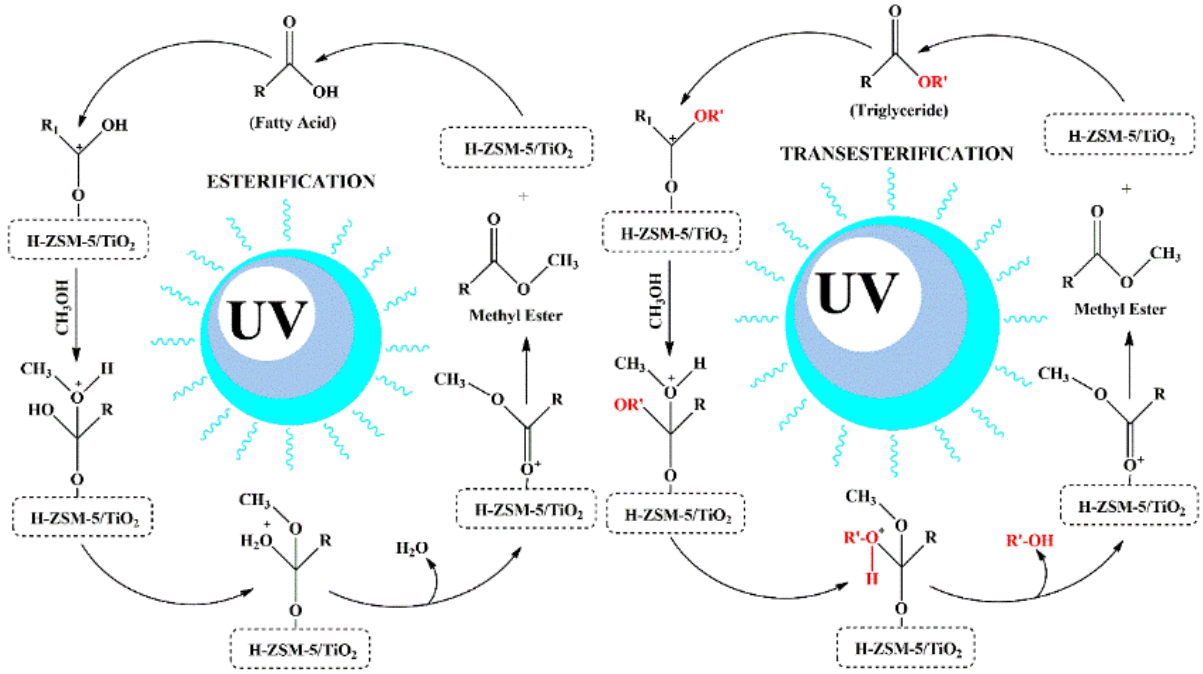

Figure 4. Esterification and Transesterification Reaction Mechanism of Tobacco Seed Oil (Voor-Oogst & Na-Oogst)(Yusur *et al.* 2023)

molecule (H_2O). This water molecule is then released (eliminated) from the structure. This is why water is often a byproduct that must be removed in biodiesel production (Da Conceicao Lobato do Nascimento *et al.*, 2025). After the water is released, the remaining structure releases protons (H+) back to the catalyst (catalyst regeneration). The result is a methyl ester (R-$COOCH_3$). The R group here represents a long carbon chain derived from tobacco seed vegetable oil.

The synthesis of methyl esters using ultrasonic waves generates small bubbles in the liquid (microcavitation), suggesting that the methoxy and ester groups in triglycerides interact to form methyl esters (biodiesel) and glycerol. The presence of TiO_2 nanoparticles in the composite, which are very active photocatalysts under UV radiation, with a large band gap energy (Liu *et al.*, 2021). The presence of this energy can rapidly and efficiently convert fatty acids and triglycerides into esters. In addition, this results in a faster formation time of methyl esters from oil and methanol using ultrasonic waves than with conventional stirring. In principle, oil and methanol are difficult to react because of the difference in molecular polarity between oil and methanol (Lin and Tseng 2024).

Figure 5. Transesterification Reaction Results

Figure 5 shows the results of the esterification and transesterification processes, which occur simultaneously (simultaneous reaction). In the synthesis of methyl ester produced with the help of ultrasonic waves with a mole ratio of oil and methanol of 1:12, the highest yield was obtained at a concentration of H-ZSM-5/TiO_2 1; 2; 3% w/w of (77.4; 84.5; 87.5)%. Then the synthesized biodiesel was compared with the 2015 SNI biodiesel, as shown in Table 2.

According to the overall fragmentation pattern analysis, the four main components of

biodiesel from synthesized tobacco seed oil are methyl palmitate (18.72%), methyl linoleate (30.76%), methyl oleate (27.26%), and methyl stearate (9.35%) (Santoso *et al.*, 2021). The successfully synthesized methyl ester has characteristic values that fall within the SNI 2015 biodiesel range, indicating that methyl ester from tobacco seed oil has the potential to be a sustainable, renewable green energy source.

Table 2. Methyl Ester Parameters and SNI Biodiesel

Parameter	Metil Ester	Biodiesel (SNI 2015)
Acid Number (mg/g)	0,46	Max 0,5
Density (g/mL)	0,865	0,850-0,890
Viscosity (cSt)	4,4	2,30-6,00

CONCLUSION

The XRD results showed that the addition of TiO2 nanoparticles did not affect the structure of H-ZSM-5. Furthermore, FTIR analysis showed that TiO_2 nanoparticles were detected at 455 and 445 cm^{-1}. After SEM-EDX Mapping testing, the nanocatalyst sample showed that TiO_2 nanoparticles were evenly distributed on the surface of H-ZSM-5, and had an average distribution of TiO_2 particles ranging from 46.07 nm. The H-ZSM-5/TiO_2 nanocatalyst exhibited outstanding catalytic activity, with acid sites contributing to its surface area, yielding the highest biodiesel yield of 87.5%. Overall, the nanocatalyst reported in this study has the potential to be used in the production of biodiesel or sustainable green energy.

ACKNOWLEDGMENTS

Thank you to the Ministry of Education, Science and Technology, and UKCW for funding and supporting basic research for novice lecturers in the 2025 budget year.

REFERENCES

Ahmad, K.A., Elahi, S.F., Znad, H., and Ahmad, E., (2025). Kinetic and mechanistic investigation of Butyl Levulinate synthesis on ZSM-5 supported phosphomolybdic acid. *Scientific Reports*, 15 (1), 1–18. https://doi.org/10.1038/s41598-025-89953-7.

Ansari, M., Jamali, H., Ghanbari, R., Ehrampoush, M.H., Zamani, P., and Hatami, B., (2025). Heterogeneous solid acid catalysts for sustainable biodiesel production from wastewater-derived sludge: A systematic and critical review. *Chemical Engineering Journal Advances*, 22 (February), 100718. https://doi.org/10.1016/j.ceja.2025.100718.

Da Conceicao Lobato do Nascimento, W., De Sousa Sousa, N., Alberto Lira Júnior, C., Dos Santos Martins, J., and Pereira Maciel, A., (2025). Study of Heterogeneous Catalysts in Transesterification for Biosiesel Production. *Revista Multidisciplinar do Nordeste Mineiro*, 2 (01), 1–16. https://doi.org/10.61164/rmnm.v2i01.3464.

Duraisamy, S., Giri, J., Rao, T.S.S.B., Kanan, M., and Manimaran, R., (2025). Optimization of cashew nut shell biodiesel production with industrial waste catalysts and butanol additives for ecofriendly CRDI engine applications. *Scientific Reports*, 15 (1), 1–29. https://doi.org/10.1038/s41598-025-93805-9.

El-Kady, K., Raslan, M., and Zaki, A.H., (2021). Effect of Different TiO_2 Morphologies on the Activity of Immobilized Lipase for Biodiesel Production. *ACS Omega*, 6 (51), 35484–35493.https://doi.org/10.1021/acsomega.1c04942.

El-Naggar, K.A., Mansor, E.S., Maafa, I.M., Abutaleb, A., Yousef, A., Matar, S.M., and Hamid, E.M.A., (2024). Valorization of marble sludge waste in biodiesel production using a central composite design. *Scientific Reports*, 14 (1), 1–20. https://doi.org/10.1038/s41598-024-77819-3.

Fatica, A., Palazzo, M., Tavaniello, S., Peng, M., Teshale, D.B., Maiorano, G., and Salimei, E., (2025). Tobacco cv. Solaris seed cake as

feed for light lambs: growth performance, carcase traits and meat quality. *Italian Journal of Animal Science*, 24 (1), 411–423. https://doi.org/10.1080/1828051X.2025.2455501.

Jit Sarma, C., Sharma, P., Bora, B.J., Bora, D.K., Senthilkumar, N., Balakrishnan, D., and Ayesh, A.I., (2023). Improving the combustion and emission performance of a diesel engine powered with mahua biodiesel and TiO_2 nanoparticles additive. *Alexandria Engineering Journal*, 72, 387–398. https://doi.org/10.1016/j.aej.2023.03.070.

Khatrin, I., Putri, D.N., Ridwan, M., and Krisnandi, Y.K., (2025). Strategic Synthesis of Hierarchical Co_3O_4/ZSM-5 Zeolite as A Catalyst in Partial Oxidation of Methane: Bottom-up vs Top-down Methods. *Bulletin of Chemical Reaction Engineering and Catalysis*, 20 (3), 505–516. https://doi.org/10.9767/bcrec.20441.

Lin, C.Y. and Tseng, S.L., (2024). Influence of Solid Alkaline Photocatalysts Irradiated with UV Light on Fuel Properties of Palm Oil Biodiesel. *ACS Omega*, 0–8. https://doi.org/10.1021/acsomega.4c04991.

Liu, Y., Yang, X., Adamu, A., and Zhu, Z., (2021). Economic evaluation and production process simulation of biodiesel production from waste cooking oil. *Current Research in Green and Sustainable Chemistry*, 4 (February), 100091.https://doi.org/10.1016/j.crgsc.2021.100091.

Matheos, C.C., Liew, D., Zomer, E., and Ademi, Z., 2023. Cost-Effectiveness Analysis of Tobacco Control Strategies in Indonesia. *Value in Health Regional Issues*, 33 (1), 65–75.

Mojapelo, N.A., Seroka, N.S., and Khotseng, L., (2025). Investigation of biomagnetic bifunctional heterogeneous nanocatalysts and cosolvents for the conversion of spent oil to biodiesel for heavy-duty transportation (jet fuel application). *Biomass and Bioenergy*, 194 (November 2024), 107664. https://doi.org/10.1016/j.vhri.2022.08.013.

Muniyappan, S. and Krishnaiah, R., (2024). The influence of TiO_2 nanoparticles on the performance, combustion, and emissions on ternary blends of n-heptane, mahua biodiesel and diesel-fuelled engine using response surface methodology. *Case Studies in Chemical and Environmental Engineering*, 10 (June), 100900. https://doi.org/10.1016/j.cscee.2024.100900.

Rajesh, K., Bibin, C., Soundararajan, G., Ashok Kumar, R., Arunkumar, S., Devarajan, Y., and Kaliappan, N., (2024). Investigating the impact of alumina nanoparticles in coconut oil distillate biodiesel to lessen emissions in direct injection diesel engine. *Scientific Reports*, 14 (1), 1–10. https://doi.org/10.1038/s41598-024-63862-7.

Santoso, A., Putri, D.E.K., Rusdi, M., Sumari-Sumari, S.S., Wijaya, A.R., and Rachman, I.B., (2021). The effect of basic catalyst concentration on tobacco oil transesterification (Voor-Oogst) using ultra-sonic wave and its potential as renewable energy. *AIP Conference Proceedings*, 2330. https://doi.org/10.1063/5.0043406.

Shinnur, M.V., Pedeferri, M.P., and Diamanti, M.V., (2024). Properties and photocatalytic applications of black TiO_2 produced by thermal or plasma hydrogenation. *Current Research in Green and Sustainable Chemistry*, 8 (May), 100415.https://doi.org/10.1016/j.crgsc.2024.100415.

Simhadri, K., Rao, P.S., and Paswan, M., (2024). Improving the combustion and emission performance of a diesel engine with TiO_2 nanoparticle blended Mahua biodiesel at different injection pressures. *International Journal of Thermofluids*, 21 (January), 100563.https://doi.org/10.1016/j.ijft.2024.100563.

Stepanov, A.A., Korobitsyna, L.L., and Vosmerikov, A. V., 2023. Investigation of the Properties of Mo/ZSM-5 Catalysts Based on Zeolites with Microporous and Micro–Mesoporous Structures. *Chemistry*

(Switzerland), 5 (2), 1256–1270. https://doi.org/10.3390/chemistry5020085.

Tshabalala, T.E., 2025. Aromatization of n-Hexane Over H- ZSM-5 and Metal (Mo , Ga , Zn) Modified H-ZSM-5 Zeolite Catalysts of Different Crystallinity Aromatization of n-Hexane Over H-ZSM-5 and Metal (Mo , Ga , Zn) Modified H-ZSM-5 Zeolite Catalysts of. *Preprints*, 1–14. doi: 10.20944/preprints202508.1327.v1.

Yang, Z., Dennis-Smither, B.J., Xu, Z., Zhao, Z., Guo, M., Sainty, N., Hou, G., Liu, X., and Sunley, G.J., (2023). Kinetic and Spectroscopic Studies of Methyl Ester Promoted Methanol Dehydration to Dimethyl Ether on ZSM-5 Zeolite. *Chemistry (Switzerland)*, 5 (1), 511–525. https://doi.org/10.3390/chemistry5010037.

Yusuf, B. O., Oladepo, S. A., & Ganiyu, S. A. (2023). Biodiesel production from waste cooking oil via β-zeolite-supported sulfated metal oxide catalyst systems. *ACS omega*, *8*(26), 23720-23732. https://doi.org/10.1021/acsomega.3c01892.

Zeleke, D.S. and Tefera, A.K., 2024. An experimental investigation of the impacts of titanium dioxide (TiO_2) and ethanol on performance and emission characteristics on diesel engines run with castor Biodiesel ethanol blended fuel. *Fuel Processing Technology*, 264 (September), 108137.https://doi.org/10.1016/j.fuproc.2024.108137.